Physica A 515 (2019) 388–402

Contents lists available at ScienceDirect

Physica A

journal homepage: www.elsevier.com/locate/physa

Multiscale joint permutation entropy for complex time series

Yi Yin [a,*], Pengjian Shang [b], Andrew C. Ahn [d,e,f], Chung-Kang Peng [c]

[a] School of Mechanical, Electronic and Control Engineering, Beijing Jiaotong University, Beijing 100044, PR China
[b] School of Science, Beijing Jiaotong University, Beijing 100044, PR China
[c] Division of Interdisciplinary Medicine and Biotechnology, Department of Medicine, Beth Israel Deaconess Medical Center, Harvard Medical School, Boston, MA 02215, USA
[d] Division for Research and Education in Complementary and Integrative Medical Therapies, Harvard Medical School, Boston, MA, 002215, USA
[e] Division of General Medicine and Primary Care, Beth Israel Deaconess Medical Center, Boston, MA 02215, USA
[f] Martinos Center for Biomedical Imaging, Massachusetts General Hospital, Boston, MA, USA

HIGHLIGHTS

- We propose MJPE method to study the synchronism between two time series.
- We apply MJPE method to the simulated time series to test the validity.
- The results show the necessity of multiscale and prove the effectiveness of MJPE.
- MJPE method is employed to the financial and traffic time series.
- MJPE results present the synchronisms from multiscale view successfully.

ARTICLE INFO

Article history:
Received 29 May 2018
Received in revised form 29 August 2018
Available online 28 September 2018

Keywords:
Multiscale joint permutation entropy (MJPE)
Synchronism
Artificial time series
Stock indices
Traffic time series

ABSTRACT

In this paper, we propose the multiscale joint permutation entropy (MJPE) to study the synchronism between two complex time series from the view of ordinal pattern and multiple scales. First, we use the Rossler system using active control, two-component ARFIMA processes to test the effectiveness of MJPE and also add some noise to the ARFIMA time series and apply MJPE to find the effect of noise. The results show the necessity of investigating the synchronism on the multiple scales, prove the effectiveness of MJPE method and show the sensitiveness of MJPE method to noise. Then MJPE method is employed to financial time series and traffic time series to validate the applicability of the proposed MJPE method for the complex time series in the real world. The conclusion from these MJPE results for financial time series is consistent with the actual situation of the synchronism and correlation between stock indices. Meanwhile, the results for traffic time series suggest the need for study the synchronism from the perspective of multiple scales and point out the different synchronisms for traffic time series of weekdays and weekends. MJPE method has a broad application prospect on the investigation of synchronism on the complex time series from different fields.

1. Introduction

Numerous techniques including Lyapunov exponent, fractal dimension and entropy, have been proposed and applied to measure the complexity of time series. Shannon proposed the concept of entropy and then various concept of entropy

* Corresponding author.
E-mail address: 09271087@bjtu.edu.cn (Y. Yin).

https://doi.org/10.1016/j.physa.2018.09.179
0378-4371/

has been developed such as approximate entropy introduced by Pincus [1–3], sample entropy developed by Richman [4,5]. Entropy not only measures the uncertainty and disorder of the time series, but also does not impose any constraints on the theoretical probability distribution [6,7]. Thus, it is very helpful to analyze complex time series. Permutation entropy (PE) is one of complexity measures which is based on comparing neighboring values of each point and mapping them to ordinal patterns [8]. Using ordinal descriptors is helpful in the sense that it adds immunity to large artifacts occurring with low frequencies. It has been proved that PE is applicable for regular, chaotic, noisy time series. Furthermore, PE has been employed to real-world time series in diverse fields such as nervous system [9], electroencephalographic (EEG) [10–13], electrocardiographic (ECG) [14,15], stock market [16] and traffic systems [17].

It is known to us that sample entropy was extended to determine the relation between two time series, by a correlation of their sample entropy, and to give a statistic termed cross sample entropy, which provides an indication of the degree of synchronizing between the signals [4]. As to PE, it is interesting and meaningful to explore how to apply the concept of PE to study the synchronism between time series. As a result, we propose the joint permutation entropy (JPE) for two time series.

Traditional entropy-based algorithms only consider one single scale. However, real-world time series from dynamical complex systems usually show multiscale structure and single scale based entropy fails to reveal the multiscale properties in the complex systems. Recently, a new entropy method termed multiscale entropy (MSE) [18–20] has been proposed and can represent the complexity over a range of scales by calculating their sample entropies. The multiscale concept resolves the contradiction that an increase of entropy may not always correspond to an increase in complexity [21]. As a result, it has been used in many different fields successfully [22–31]. In this paper, we further combine JPE with the concept of multiscale and propose the multiscale joint permutation entropy (MJPE) in this paper to detect the properties between two complex time series from the view of ordinal pattern and multiple scales.

The reminder of the paper is organized as follows. Section 2 briefly introduces the multiscale joint permutation entropy we proposed. In Section 3, we use simulated time series to test the effectiveness of MJPE and study the effect of noise to MJPE. Applications to the financial time series and traffic time series are presented in Section 4. Finally, we offer concluding remarks in Section 5.

2. Multiscale joint permutation entropy

We develop PE into MJPE to study the multiscale structure of the synchronism between time series. Consider two time series $\{x_t, t = 1, 2, \ldots, N\}$ and $\{y_t, t = 1, 2, \ldots, N\}$, where N is the equal length of the time series. Then we construct the coarse-grained dimensional time series $\{X_k^s\}$ and $\{Y_k^s\}$ as

$$\begin{aligned} X_k^s &= \frac{1}{s}\sum_{t=(k-1)s+1}^{ks} x_t \\ Y_k^s &= \frac{1}{s}\sum_{t=(k-1)s+1}^{ks} y_t \end{aligned} \tag{1}$$

where s represents the scale factor and $1 \le k \le M = N/s$. The length of each coarse grained time series is equal to the length of original time series divided by the scale factor s. First we calculate joint permutation entropy for these coarse grained time series as following procedure. For the coarse grained time series $\{X_k^s\}$ and $\{Y_k^s\}$, we construct their time-delay embedding representations $Z_{1,l}^{d,\tau,s} = \{X_l^s, X_{l+\tau}^s, \ldots, X_{l+(d-1)\tau}^s\}$ and $Z_{2,l}^{d,\tau,s} = \{Y_l^s, Y_{l+\tau}^s, \ldots, Y_{l+(d-1)\tau}^s\}$ for $l = 1, 2, \ldots, M-(d-1)\tau$,where d and τ denote the embedding dimension and time delay, respectively. To compute JPE, each of the $T = M-(d-1)\tau$ subvectors is assigned a single motif out of $d!$ possible ones (representing all unique orderings of d different numbers). Thus, when we calculate the joint frequencies which denote the probability that the two time series have the certain motif respectively at the same time, there are $d! \times d!$ possible conditions. For example, if we choose the embedding dimension as 3, there are 6 motifs for each time series as shown in Fig. 1 and 36 different possible motif combinations.

JPE is then defined as the Shannon entropy of the $d! \times d!$ distinct motif combinations $\{(\pi_i^{d,\tau}, \pi_j^{d,\tau})\}$, denoted as Π:

$$JPE(d, \tau) = -\sum_{i,j:(\pi_i^{d,\tau}, \pi_j^{d,\tau})} p(\pi_i^{d,\tau}, \pi_j^{d,\tau}) ln p(\pi_i^{d,\tau}, \pi_j^{d,\tau}) \tag{2}$$

$p(\pi_i^{d,\tau}, \pi_j^{d,\tau})$ is defined as

$$p(\pi_i^{d,\tau}, \pi_j^{d,\tau}) = \frac{\|l : l \le T, type(Z_{1,l}^{d,\tau,s}, Z_{2,l}^{d,\tau,s}) = (\pi_i^{d,\tau}, \pi_j^{d,\tau})\|}{T} \tag{3}$$

where $type(\cdot)$ denotes the map from pattern space to symbol space and $\|\cdot\|$ denotes the cardinality of a set. The maximum value of JPE is $ln(d! \times d!)$, which implies that all motif combinations have an equal probability. The smallest value of JPE is zero, which implies it is a mere repetition of the same basic motif combination. Thus JPE varies in the range $[0, ln(d! \times d!)]$ and is

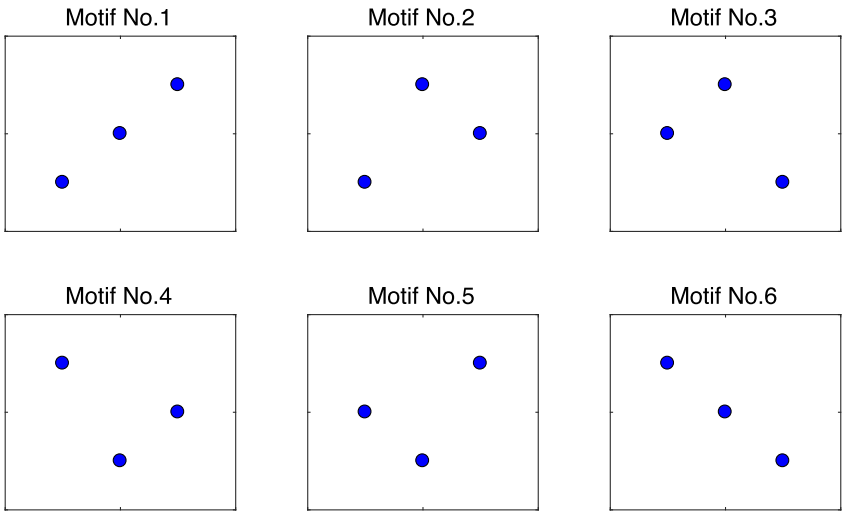

Fig. 1. The six different motifs for each time series when the embedding dimension is choose as 3.

invariant under nonlinear monotonic transformations. For convenience, we normalize JPE by its maximum value $ln(d! \times d!)$:

$$0 \leq \frac{JPE(d, \tau)}{ln(d! \times d!)} \leq 1 \tag{4}$$

Besides, we also define a variance to measure the correlation between these series as follow

$$variance\_JPE(d, \tau) = \sum_{i,j:(\pi_i^{d,\tau}, \pi_j^{d,\tau})} [p(\pi_i^{d,\tau}, \pi_j^{d,\tau}) - p(\pi_i^{d,\tau}, \cdot) \times p(\cdot, \pi_j^{d,\tau})] \tag{5}$$

where $p(\pi_i^{d,\tau}, \cdot)$ denotes the probability of the first time series has the ith motif regardless of the second time series, while $p(\cdot, \pi_j^{d,\tau})$ denotes the probability of the second time series has the jth motif regardless of the first time series. Then after the calculation of the normalized JPE for each coarse grained time series we obtain the MJPE with scale factor s and then plot the MJPE. The variance of MJPE is also obtained. It can be seen from Eq. (3), (5) that the MJPE value is bigger which indicates the synchronism between time series is lower and the variance is smaller which shows the correlation between time series is lower. The embedding dimension d decides the number of accessible states and thus plays an important part in estimating the joint permutation probability distribution P. Similar as the previous study on PE, the choice of d depends on the length N of the time series, in such a way that the constraint $(d! \times d!) \ll N$ must be satisfied in order to obtain reliable statistics. Bandt and Pompe [8] recommend $d = 3, 4, \ldots, 7$ in the PE method for practical purposes when the constraint is $d! \ll N$. Besides, increasing embedding dimension d affects the running time without significantly changing the obtained entropies. Hence, without loss of generality, we choose the embedding dimensions d as 3 for simplicity and convenience. Meanwhile, the time delay τ is chosen as 1 in order to avoid cross effects.

3. Numerical experiments for artificial time series

Before discussing multiscale analysis of practical time series and its interpretation, we illustrate MJPE method to simulated examples where a judgment can be made about the validity and accuracy of the method. In this section, we use artificial time series including Rossler systems using active control, two-exponent ARFIMA processes to test the effectiveness of the method and the effect of noise to the MJPE method.

3.1. Rossler systems using active control

First, we apply MJPE to the Rossler system without and with active control [32–37]. The Rossler system [34] is described by the set of ordinary differential equations

$$\begin{aligned} \dot{x} &= -y - z, \\ \dot{y} &= x + ay, \\ \dot{z} &= b + z(x - c) \end{aligned} \tag{6}$$

In this paper, we assume that we have two Rossler systems and that the drive system with the subscript 1 is to control the response system with subscript 2. The drive and response systems are defined as follows:

$$\begin{aligned} \dot{x_1} &= -y_1 - z_1, \\ \dot{y_1} &= x_1 + ay_1, \\ \dot{z_1} &= b + z_1(x_1 - c) \end{aligned} \tag{7}$$

and

$$\begin{aligned} \dot{x_2} &= -y_2 - z_2 + u_1(t), \\ \dot{y_2} &= x_2 + ay_2 + u_2(t), \\ \dot{z_2} &= b + z_2(x_2 - c) + u_3(t) \end{aligned} \tag{8}$$

The response system (8) introduces three control functions $u_1(t)$, $u_2(t)$ and $u_3(t)$ and we subtract (7) from (8) in order to estimate the control functions.

$$\begin{aligned} x_3 &= x_2 - x_1, \\ y_3 &= y_2 - y_1, \\ z_3 &= z_2 - z_1 \end{aligned} \tag{9}$$

Then an error system is defined as the differences between the Rossler systems (7) and (8). Using this notation, we obtain the error system as follow

$$\begin{aligned} \dot{x_3} &= -y_3 - z_3 + u_1(t), \\ \dot{y_3} &= x_3 + ay_3 + u_2(t), \\ \dot{z_3} &= x_2z_2 - x_1z_1 - cz_3 + u_3(t) \end{aligned} \tag{10}$$

x_3, y_3 and z_3 are called the error states. We can get the synchronization between the Rossler systems by using the control functions to achieve the asymptotic stability of the zero solution of the error system (10). The active control functions $u_1(t)$, $u_2(t)$ and $u_3(t)$ are defined as follows:

$$\begin{aligned} u_1(t) &= V_1(t), \\ u_2(t) &= V_2(t), \\ u_3(t) &= x_1z_1 - x_2z_2 + V_3(t) \end{aligned} \tag{11}$$

So the error system (10) changes into

$$\begin{aligned} \dot{x_3} &= -y_3 - z_3 + V_1(t), \\ \dot{y_3} &= x_3 + ay_3 + V_2(t), \\ \dot{z_3} &= -cz_3 + V_3(t) \end{aligned} \tag{12}$$

There are many possible choices for the control $V_1(t)$, $V_2(t)$ and $V_3(t)$. We choose

$$\begin{pmatrix} V_1(t) \\ V_2(t) \\ V_3(t) \end{pmatrix} = A \begin{pmatrix} x_3 \\ y_3 \\ z_3 \end{pmatrix} \tag{13}$$

where A is a 3×3 constant matrix. In order to make the closed loop system will be stable, the proper choice of the elements of the matrix A is such that the feedback system must have all of the eigenvalues with negative real parts. In this paper the matrix A is chosen in the form (14) which makes the closed loop system (12) have the eigenvalues -1, -1 and -1.

$$A = \begin{pmatrix} -1 & 1 & 1 \\ -1 & -(1+a) & 0 \\ 0 & 0 & c-1 \end{pmatrix} \tag{14}$$

With this choice, the error states x_3, y_3 and z_3 will converge to zero as time t tends to infinity and hence achieve the synchronization of drive and response systems.

According to the paper [35], we choose numerical values for the parameters in (6) as $a = 0.2, b = 0.2, c = 5.7$ to insure the chaotic behavior of Rossler system. We use fourth-order Runge–Kutta method to solve the systems of differential Eqs. (7) and (8) with time step size equal 0.001 in these numerical simulations. The initial values of the drive system are $x_1(0) = 0.5, y_1(0) = 1, z_1(0) = 1.5$ and the initial values of the response system are $x_2(0) = 2.5, y_2(0) = 2, z_2(0) = 2.5$. Then the initial values for the error states are $x_3(0) = 2, y_3(0) = 1, z_3(0) = 1$. Based on these parameters and initial values, we can obtain the identical Rossler system without active control and with active control. We apply the MJPE method to the

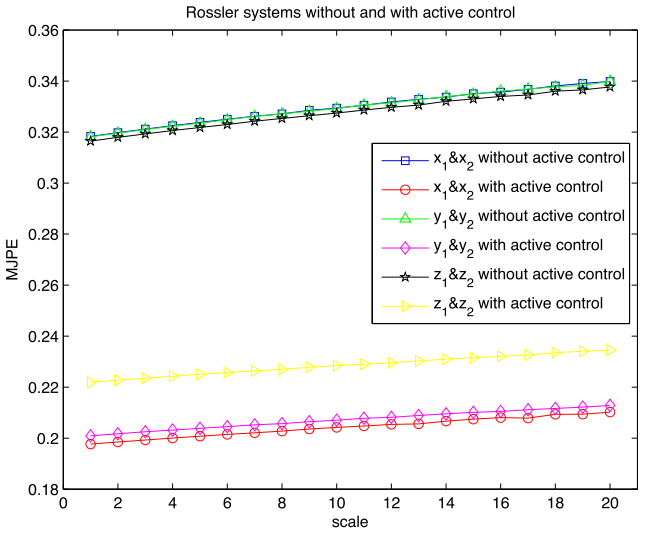

Fig. 2. MJPE results for the two identical Rossler systems without and with active control.

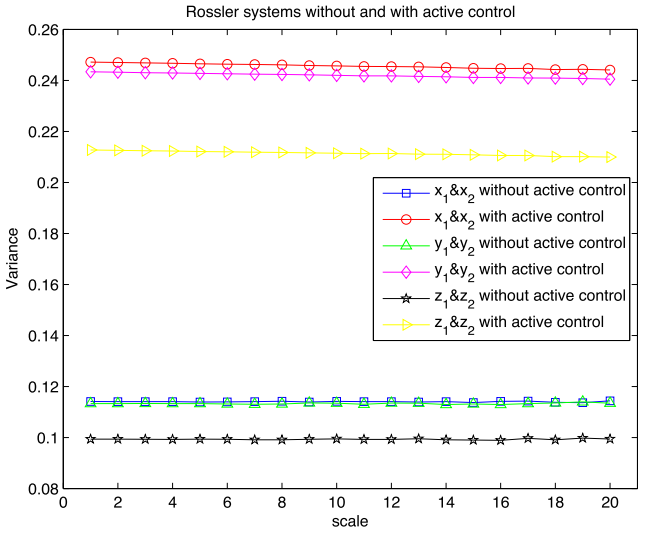

Fig. 3. Variance of MJPE for the two identical Rossler systems without and with active control.

time series x_1&x_2 without active control, x_1&x_2 with active control, y_1&y_2 without active control, y_1&y_2 with active control, z_1&z_2 without active control, z_1&z_2 with active control, and their MJPE results and variance of MJPE are shown in Figs. 2, 3, respectively. It can be found that MJPE results for the Rossler systems with active control are lower than those for the Rossler systems without active control, which means higher synchronism. Variances of MJPE also show stronger correlation for the Rossler systems with active control. It confirms the fact that using active control achieves the synchronization between Rossler systems and presents the effectiveness of MJPE.

3.2. Two-component ARFIMA process

The power-law auto-correlations in stochastic variables can be modeled by an ARFIMA process [38,39]:

$$z(t) = Z(d, t) + \varepsilon_z(t) \tag{15}$$

where $d \in (0, 0.5)$ is a memory parameter, ε_z is an independent and identically distributed Gaussian variable, and $Z(d, t) = \sum_{n=1}^{\infty} a_n(d) z(t-n)$, in which $a_n(d) = d\Gamma(n-d)/[\Gamma(1-d)\Gamma(n+1)]$ is the weight. The Hurst index H_{zz} is related to the memory parameterized by [40,41]. For the two-component ARFIMA processes discussed below, we take $Z = X$ or Y.

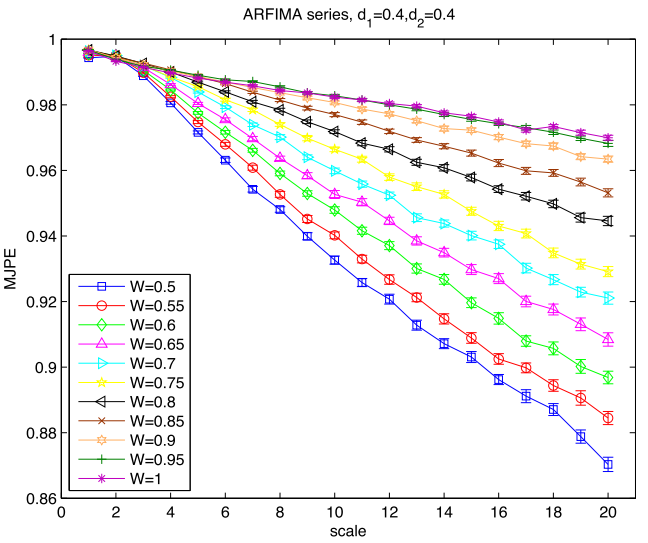

Fig. 4. MJPE results for the series simulated by two-component ARFIMA process with $d_1 = d_2 = 0.4$ and W from 0.5 to 1.

The two-component ARFIMA process is defined as follows [40]:

$$\begin{cases} x(t) = WX(d_1, t) + (1 - W)Y(d_2, t) + \varepsilon_x(t) \\ y(t) = (1 - W)X(d_1, t) + WY(d_2, t) + \varepsilon_y(t) \end{cases} \tag{16}$$

where $W \in [0.5, 1]$ quantifies the coupling strength between the two processes $x(t)$ and $y(t)$. The cross-correlation between two processes $x(t)$ and $y(t)$ decreases with the increasing W from 0.5 to 1[38]. When W increases to 1, $x(t)$ and $y(t)$ are fully decoupled and become two separate ARFIMA processes as defined in Eq. (15).

Without loss of generality, we choose $W = 0.8$ and the parameters (d_1, d_2) of ARFIMA as $d_1 = d_2 = 0.4$ and $d_1 = 0.1$, $d_2 = 0.4$ separately, and corresponding two error terms $\varepsilon_x(t)$ and $\varepsilon_y(t)$ share one independent and identically distributed Gaussian variable with zero mean and unit variance. We apply MJPE method to the series simulated by two-component ARFIMA process. Figs. 4, 5 show MJPE and variance of MJPE between the series simulated by two-component ARFIMA process with $d_1 = d_2 = 0.4$, W from 0.5 to 1, while Figs. 6, 7 present MJPE and variance of MJPE results between the series simulated by two-component ARFIMA process with $d_1 = 0.1, d_2 = 0.4$, W from 0.5 to 1, respectively. The numerical results are quantified by calculating 100 pairs of independent ARFIMA series with $d_1 = d_2 = 0.4$ and $d_1 = 0.1, d_2 = 0.4$ separately. Because 100 pairs of independent ARFIMA series are used and each series contains 4096 data points, we can obtain the means and standard errors of entropy and variance values which have been shown in Figs. 4–7. It can be seen from Figs. 4, 6 that the MJPE results become larger when W increases from 0.5 to 1 indicating the synchronism between these time series become lower. Meanwhile, the variances of MJPE in Figs. 5, 7 get lower when W increases from 0.5 to 1. Moreover, MJPE results of ARFIMA series with W from 0.5 to 1 are similar when scale changes from 1 to 3 in Figs. 4, 6, while variance of MJPE of ARFIMA series with W from 0.5 to 1also show the similarity when scale changes from 1 to 3 in Figs. 5, 7. It suggests necessity of investigating the synchronism on the multiple scales. Both behaviors of MJPE and variance of MJPE are consistent with the fact that synchronism and correlation decrease when W increases from 0.5 to 1, which means MJPE method is applied to ARFIMA series to detect the synchronism on multiple scales 1–20 successfully.

Then we add some noises to the ARFIMA time series and apply MJPE to find the effect of noise on the results. Without loss of generality, we use the series simulated by two-component ARFIMA process with $d_1 = d_2 = 0.4$, $W = 0.5$ as an example. Some white noise is added to one of the ARFIMA series and the percentage of noise changes from 10% to 100% with step 10%. The MJPE and variance of MJPE for these time series are shown in Figs. 8, 9, respectively. It is obvious to find that the MJPE becomes larger and variance of MJPE becomes smaller when percentage of noise increases, which also prove the effectiveness of MJPE method and show the sensitiveness of MJPE method to noise.

4. Analysis for the real-world time series

In order to validate the applicability of the proposed MJPE method for the complex time series in the real world, we then apply MJPE method to financial time series and traffic time series.

4.1. Analysis for financial time series

Recently, stock markets have become active areas and attracted much attention. Stock market indices are important measures of financial and economical performance and are normally used to benchmark the performance of stock portfolios.

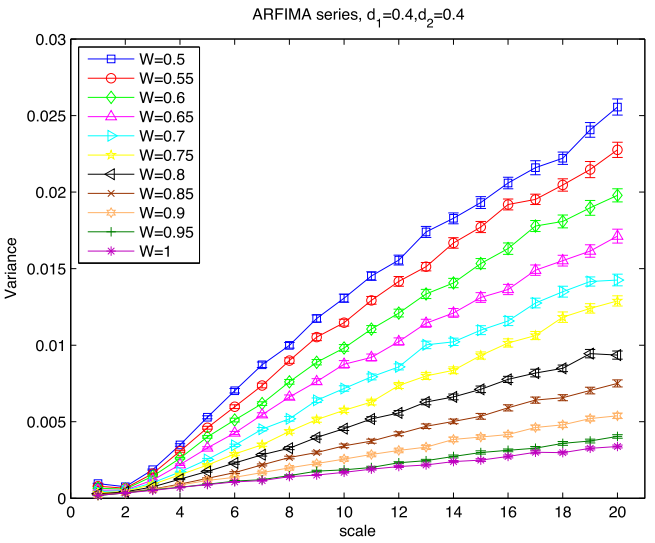

Fig. 5. Variance of MJPE for the series simulated by two-component ARFIMA process with $d_1 = d_2 = 0.4$ and W from 0.5 to 1.

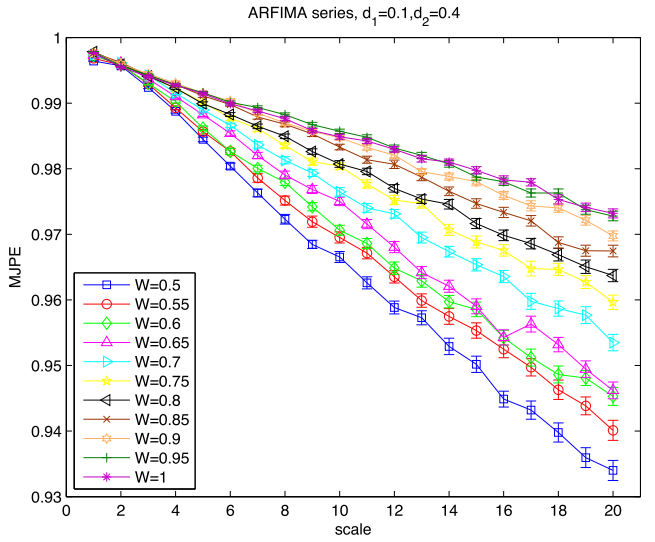

Fig. 6. MJPE results for the series simulated by two-component ARFIMA process with $d_1 = 0.1$, $d_2 = 0.4$ and W from 0.5 to 1.

The study of the international stock markets is attractive for both fundamental and practical researches. On the fundamental side, a financial market has been referred to as an example of a complex system consisting of many interacting components. An abrupt variant on a certain component can be spatially affected by the others as well as itself temporally. Statistical motivations are to visualize correlations in order to suggest some potentially plausible parameter relations and restrictions. On the practical side, economic motivations are to identify the main factors which affect the behavior of stock markets across different exchanges and countries. Moreover, it is important for evaluating the risk of an investment in the stock market. The understanding of such relations would be helpful to design good portfolios [42,43]. It is therefore of great interest to analyze the synchronisms embedded in international stock markets.

In this paper, we use the daily price return of six stock indices including three US stock indices (S&P500, DJI, NQCI) and three Chinese stock indices (ShangZheng(SZ), ShenCheng(SC), HSI) from January 3, 1997, to December 28, 2012. In order to make these indices have the same opening dates and obtain the same length time series, we exclude the asynchronous data and then reconnect the remaining parts of the original series. As a result, the total of the closing prices recorded is 3572 days. Generally, the daily price return r_t is used to investigate the time series of stock market. It is calculated as the logarithmic difference of the closing price, i.e. $r_t = log(x_t) - log(x_{t-1})$ where x_t denotes the closing price for a stock index on day t. The daily price returns of six stock indices are shown in Fig. 10.

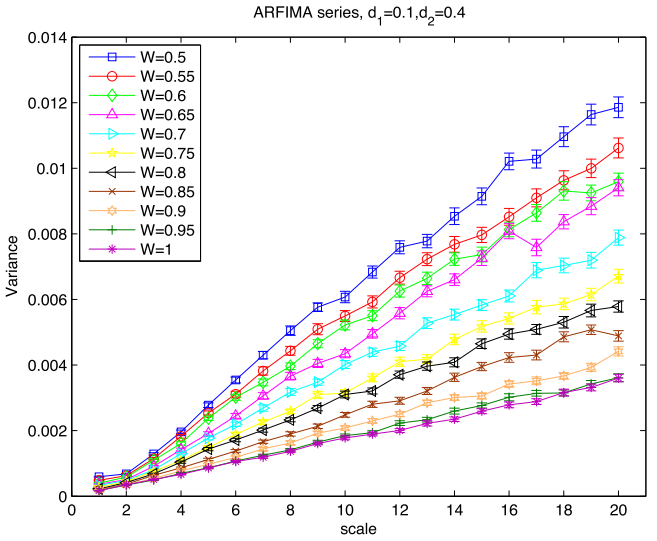

Fig. 7. Variance of MJPE for the series simulated by two-component ARFIMA process with $d_1 = 0.1$, $d_2 = 0.4$ and W from 0.5 to 1.

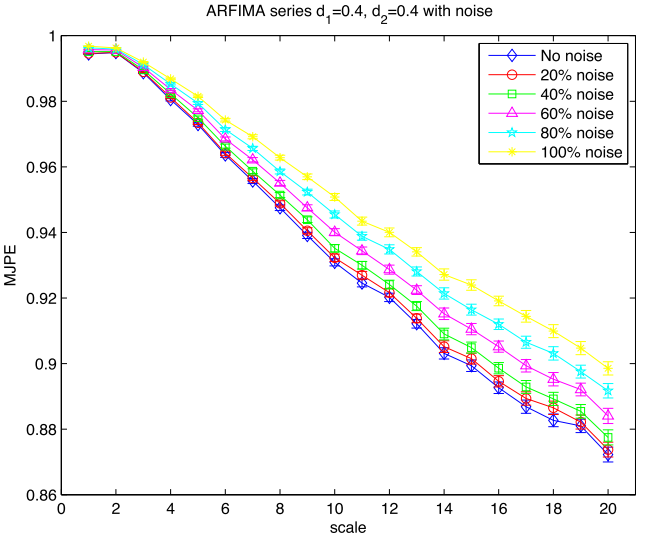

Fig. 8. MJPE results for the series simulated by two-component ARFIMA process with $d_1 = d_2 = 0.4$, $W = 0.5$ with different percent of noise from 10% to 100%.

We apply the MJPE method to these time series and present the MJPE results and variance of MJPE for the stock indices in the same region: S&P500&DJI, S&P500&NQCI, DJI&NQCI (US), and SZ&HSI, SC&HSI, SZ&SC (China) in Figs. 11, 12. For US stock markets, the MJPE for S&P500&DJI fluctuates in the range (0.7, 0.75), the MJPE for S&P500&NQCI fluctuates in the range (0.72, 0.8) and the MJPE for DJI&NQCI fluctuates around 0.85. For Chinese stock markets, the MJPE for SZ&HSI, SC&HSI fluctuate in the range (0.95, 1) and the MJPE for SZ&SC varies from 0.72 to 0.79. The MJPE for SZ&HSI, SC&HSI are larger than the others, while their variances of MJPE are smaller than the others, which means the synchronism of SZ&HSI, SC&HSI is smaller. The MJPE and variance of MJPE for DJI&NQCI are different from the other three which shows a smaller synchronism. Meanwhile, the MJPE and variance of MJPE for S&P500&DJI, S&P500&NQCI, SZ&SC show their synchronisms are larger. Then the MJPE method is employed to study the synchronism for the stocks markets between US and China: S&P500&SZ, S&P500&SC, S&P500&HSI, DJI&SZ, DJI&SC, DJI&HSI, NQCI&SZ, NQCI&SC, NQCI&HSI and their results are shown in Figs. 13, 14. MJPE results for S&P500&SZ, S&P500&SC, DJI&SZ, DJI&SC, NQCI&SZ, NQCI&SC are similar and larger than those for S&P500&HSI, DJI&HSI, NQCI&HSI, while their variances of MJPE are similar and smaller than those for S&P500&HSI, DJI&HSI, NQCI&HSI as well. It can be found that the synchronisms between HSI and US stock markets are higher, while the synchronisms between HSI and stock markets in Chinese mainland, which is consistent with the actual situations that the US stock markets have stronger influence on the stock markets in Hong Kong than in Chinese mainland. Meanwhile, by comparing the MJPE results

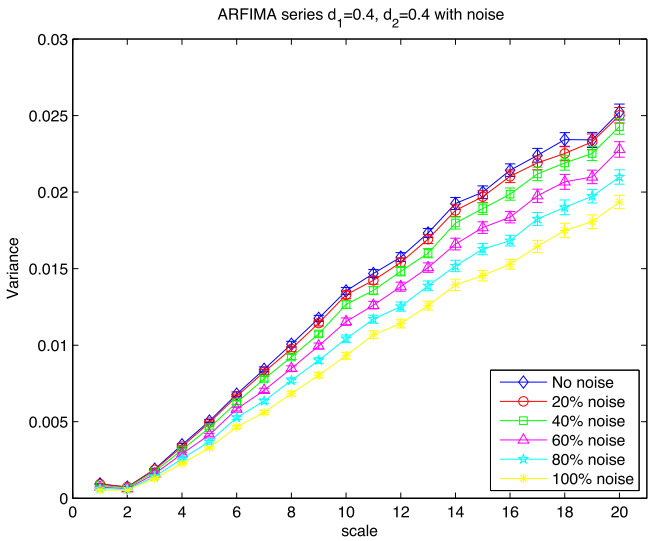

Fig. 9. Variance of MJPE for the series simulated by two-component ARFIMA process with $d_1 = d_2 = 0.4$, $W = 0.5$ with different percent of noise from 10% to 100%.

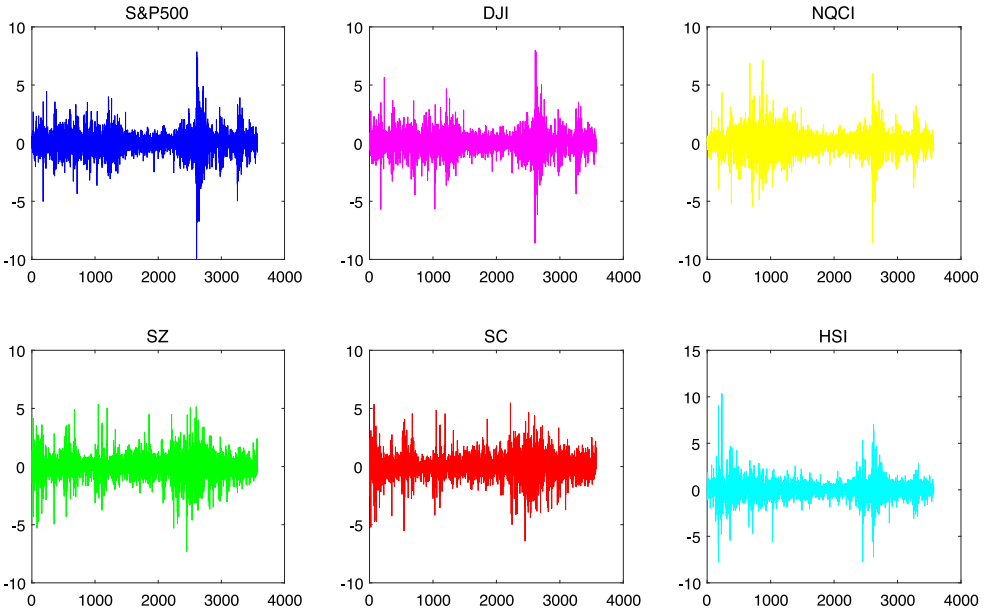

Fig. 10. Daily price returns for the S&P500, DJI, NQCI, SZ, SC, and HSI stock indices.

in Figs. 11 and 13, we find the MJPE results in the same region are smaller than the MJPE results in the different region. It is consistent with the conclusion obtained in previous studies [44–49] that the stock indices from the same region have larger synchronism. Besides, it can be found that the MJPE and variance of MJPE for the stock indices in the same region fluctuate with the scale s, while the MJPE for the stock indices in the different regions decrease with scale s and their variance of MJPE increase with scale s, which shows there are different inner mechanisms of the synchronism for different regions.

4.2. Analysis for traffic time series

The study engaged in the traffic systems has developed rapidly in recent years. The reasons for the rapid development can be listed as follows: The first is the current state of mathematical models for relationship between traffic volume and speed is in a state of flux [50–55], and the models that dominated the discourse are incompatible with the data that is currently being obtained by advanced intelligent transportation systems (ITS) technologies, the second is the various

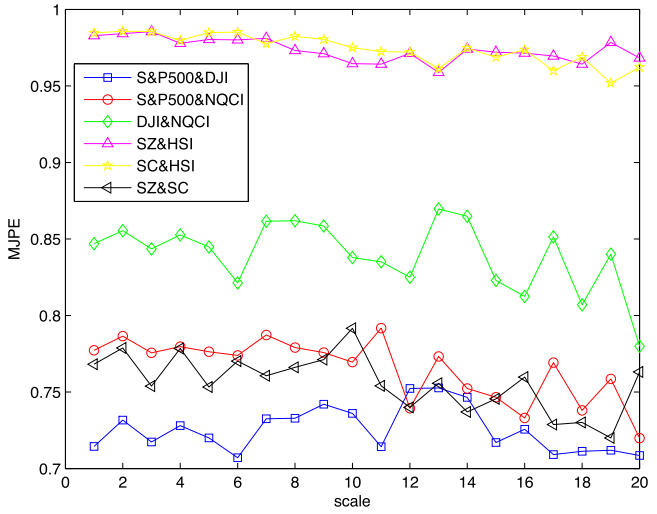

Fig. 11. MJPE results for the stocks markets in the same region: S&P500&DJI, S&P500&NQCI, DJI&NQCI (US), and SZ&HSI, SC&HSI, SZ&SC (China).

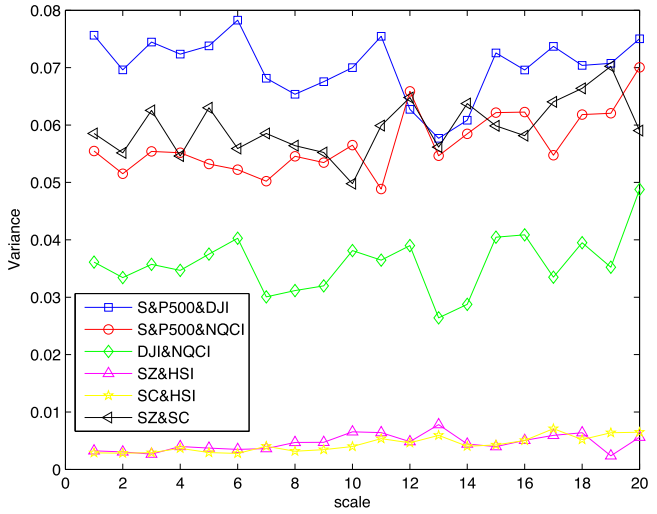

Fig. 12. Variance of MJPE for the stocks markets in the same region: S&P500&DJI, S&P500&NQCI, DJI&NQCI (US), and SZ&HSI, SC&HSI, SZ&SC (China).

nonlinear dynamical phenomena, such as the formation of fractal and chaos, are observed [56–64]. A great number of empirical studies have shown that the traffic system is a typically complex system in terms of system engineering [58,59]. Considerable interest in fields as diverse as mechanics, mathematics, physics, engineering science, and psychology have been attracted in interdependent behavior and causality in traffic complex systems. In the past few years, there are a lot of different methods which have been used on the transportation research, including complex network [65], chaotic analysis method [60] and nonlinear method [61], to investigate the traffic complex system. To detect the synchronism and intrinsic nature of traffic system will be meaningful and necessary to get a better understanding of the complex traffic system dynamics and mechanism and lay a solid theoretical basis to establish the advanced intelligent urban traffic management and control strategy and technology which can further improve traffic conditions efficiently.

People are more concerned about traffic information in metropolises such as Beijing, where the road condition deeply affects the quality of life of residents and the social economy. Traffic systems have numerous parameters that can be measured, such as the traffic volume, speed and occupancy. In this paper, we apply MJPE on the traffic speed and volume time series on lane 1, which are collected from detectors 2036 to 2037 lying on the West 2nd Ring Road (Beijing, China) over a period of about 11 weeks, from August 11 to October 26, 2012. The detectors record the raw data every 20 s and then aggregate the raw data into two-minute data for average. Thus, the one-hour recorded traffic time series are about 30 data points, and the total number of data points for the whole series is about 55 440. It is known that there are two important patterns: (i) weekday pattern, and (ii) weekend pattern for traffic time series. Fig. 15 show part of speed series on lane 1 recorded by detector 2036 shown for example (upper panel) and one-day series of speed on lane 1 at weekday and weekend

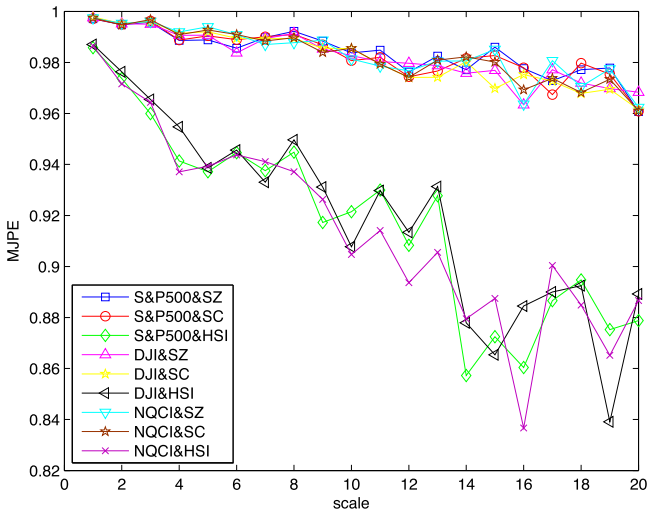

Fig. 13. MJPE results for the stocks markets between US and China: S&P500&SZ, S&P500&SC, S&P500&HSI, DJI&SZ, DJI&SC, DJI&HSI, NQCI&SZ, NQCI&SC, NQCI&HSI.

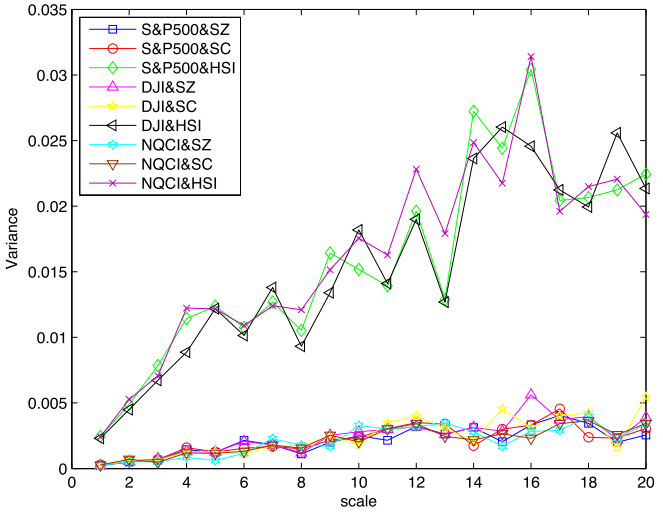

Fig. 14. Variance of MJPE for the stocks markets between US and China: S&P500&SZ, S&P500&SC, S&P500&HSI, DJI&SZ, DJI&SC, DJI&HSI, NQCI&SZ, NQCI&SC, NQCI&HSI.

separately (lower panel). It can be found from the lower panel of Fig. 15 that the speed series at weekday shows two sudden drop at rush hours, which represents the periodic pattern of weekday and may affect the synchronism. Thus, we consider the differences between the synchronisms for these traffic series on whole weeks, separate weekdays and separate weekends. Figs. 16, 17 display the MJPE and variance of MJPE for the speed time series and volume time series on lane 1 recorded by detector 2036 of whole weeks, weekdays and weekends, while MJPE and variance of MJPE for the speed time series on lane 1 recorded by detector 2036 and 2037 of whole weeks, weekdays and weekends are shown in Figs. 18, 19, respectively. For the MJPE and variance of MJPE of both between speed and volume and the speed time series between adjacent detectors, the results show no differences at the small scales and become distinct at larger scales suggesting the need for study the synchronism from the perspective of multiscale. The results also point out that the synchronisms for traffic time series of weekdays are different from that those of weekends and the synchronisms for weekday are smaller than those for weekends. Meanwhile, the synchronisms for traffic time series of whole week are between those of weekdays and weekends, but much closer to those of weekdays. All of these synchronisms increase with the increase of scale s. MJPE is capable of reflecting the difference on synchronisms due to weekday patterns and weekend patterns.

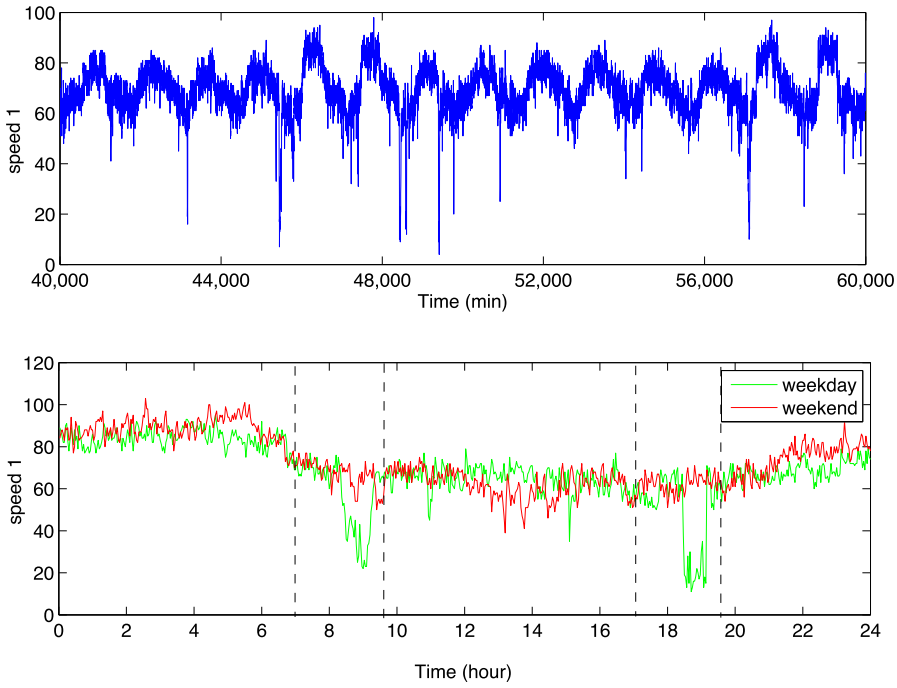

Fig. 15. Part of speed series on lane 1 recorded by detector 2036 shown for example (upper panel) and one-day series of speed on lane 1 at weekday and weekend separately (lower panel).

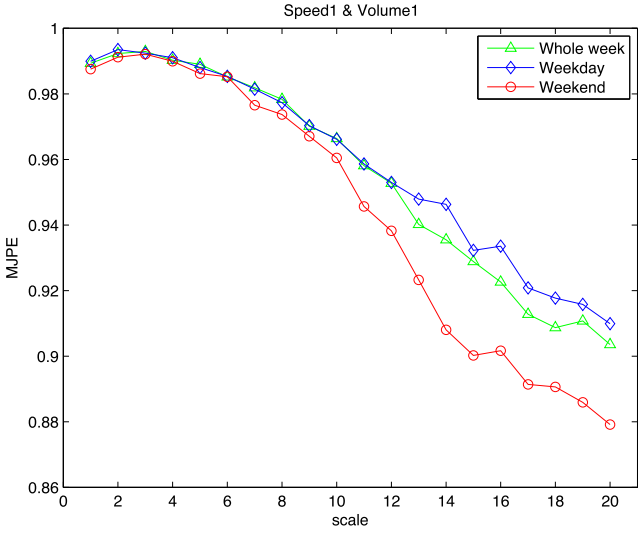

Fig. 16. MJPE results for speed time series and volume time series on lane 1 recorded by detector 2036 of whole weeks, weekdays and weekends.

5. Conclusions

In this paper, we introduce the concept of PE to the study between two time series and then combine with the concept of multiscale. Thus, we propose the multiscale joint permutation entropy (MJPE) to study the synchronism between two complex time series from the view of ordinal pattern and multiple scales. Before discussing multiscale analysis of practical time series and its interpretation, we illustrate MJPE method to simulated examples: Rossler systems without and with active control, two component ARFIMA series without and with noise to show the validity of this method. The results for Rossler systems confirm the fact that using active control achieves the synchronization between Rossler systems and presents the effectiveness of MJPE. For the ARFIMA time series, their results are consistent with the fact that synchronism and correlation decrease when W increases from 0.5 to 1, which means MJPE method is applied to ARFIMA series to detect the synchronism

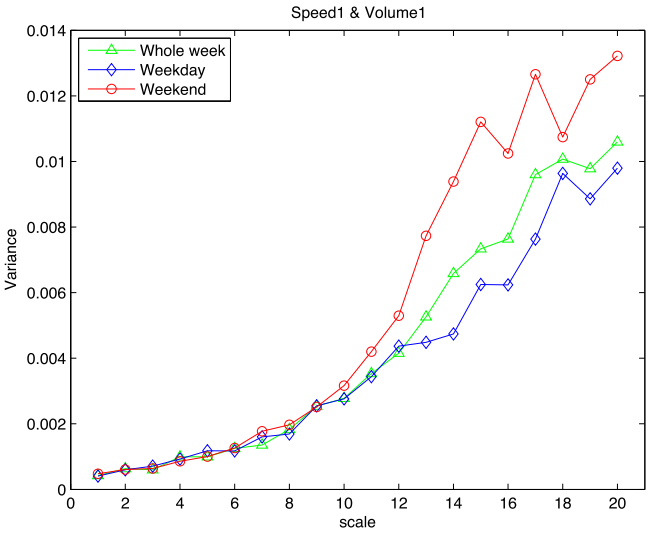

Fig. 17. Variance of MJPE for speed time series and volume time series on lane 1 recorded by detector 2036 of whole weeks, weekdays and weekends.

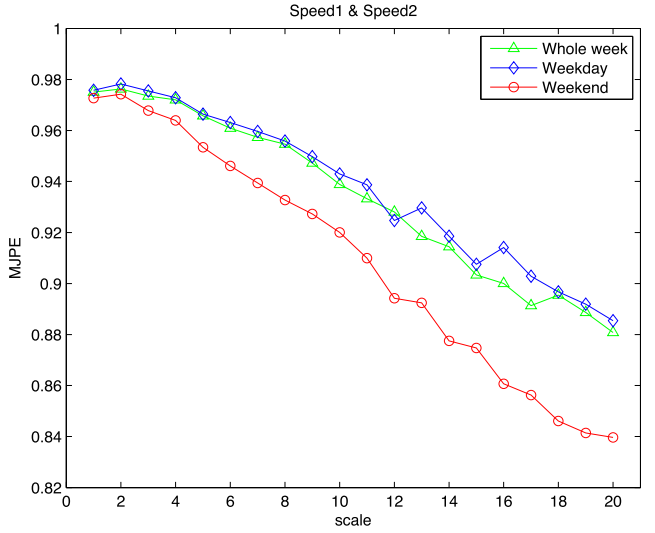

Fig. 18. MJPE results for speed time series on lane 1 recorded by detector 2036 and 2037 of whole weeks, weekdays and weekends.

on multiple scales 1–20 successfully. Meanwhile, the results for the ARFIMA time series with different percentage of noise also prove the effectiveness of MJPE method and show the sensitiveness of MJPE method to noise. Then we apply the MJPE method to the complex time series in the real world: financial time series and traffic time series. The conclusion drawn from the MJPE results for financial time series is consistent with the actual situation that the stock indices from the same region have larger synchronism and the US stock markets have stronger influence on the stock markets in Hong Kong than Chinese mainland. Besides, it also shows there is different inner mechanism of the synchronism for different regions. The analysis of traffic time series indicates the need for study the synchronism from the perspective of multiscale and the differences between the synchronisms for these traffic series on whole weeks, separate weekdays and separate weekends. MJPE method can be applied to the complex time series from various fields. In the future, we intend to use MJPE method on the study of biological time series such as EEG signals, ECG signals. It can be very helpful on exploring the change of synchronism with age, diseases, sleep stage etc. and further meaningful for the clinical diagnosis.

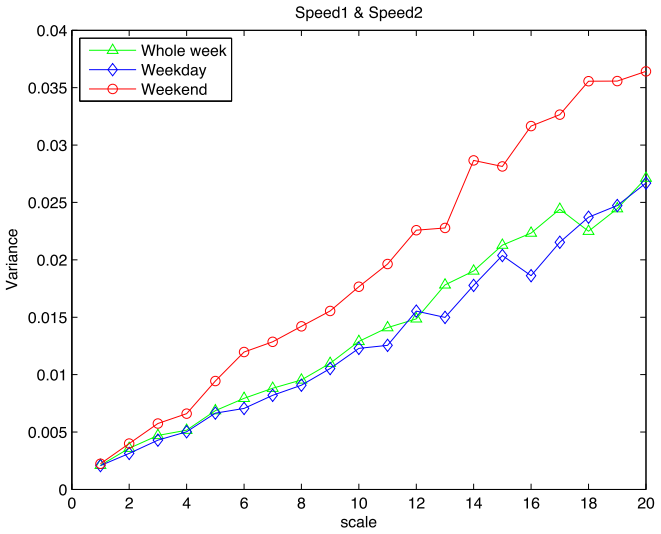

Fig. 19. Variance of MJPE for speed time series on lane 1 recorded by detector 2036 and 2037 of whole weeks, weekdays and weekends.

References

[1] S.M. Pincus, Approximate entropy as a measure of system complexity, Proc. Natl. Acad. Sci. USA 88 (1991) 2297–2301.
[2] S.M. Pincus, Approximate entropy (ApEn) as a complexity measure, Chaos 5 (1995) 110–117.
[3] S.M. Pincus, Quantifying complexity and regularity of neurobiological systems, Meth. Neurosci. 28 (1995) 336–363.
[4] J.S. Richman, J.R. Moorman, Physiological time-series analysis using approximate entropy and sample entropy, Amer. J. Physiol. Heart Circ. Physiol. 278 (2000) 2039–2049.
[5] D.E. Lake, J.S. Richman, M.P. Griffi, J.R. Moorman, Sample entropy analysis of neonatal heart rate variability, Am. J. Physiol. Regul. Integr. Comp. Physiol. 283 (2002) 789–797.
[6] G.A. Darbellay, D. Wuertz, The entropy as a tool for analysing statistical dependences in financial time series, Physica A 287 (2000) 429–439.
[7] S.R. Bentes, R. Menezes, D.A. Mendes, Long memory and volatility clustering: is the empirical evidence consistent across stock markets? Physica A 387 (2008) 3826–3830.
[8] C. Bandt, B. Pompe, Permutation entropy: A natural complexity measure for time series, Phys. Rev. Lett. 88 (2002) 174102.
[9] Z. Li, G. Ouyang, D. Li, X. Li, Characterization of the causality between spike trains with permutation conditional mutual information, Phys. Rev. E 84 (2011) 021929.
[10] X. Li, S. Cui, L. Voss, Using permutation entropy to measure the electroencephalographic effects of sevoflurane, Anesthesiology 109 (2008) 448–456.
[11] X. Li, G. Ouyang, D. Richards, Predictability analysis of absence seizures with permutation entropy, Epilepsy Res. 77 (2007) 70–74.
[12] A. Bruzzo, B. Gesierich, M. Santi, C. Tassinari, N. Birbaumer, G. Rubboli, Permutation entropy to detect vigilance changes and preictal states from scalp EEG in epileptic patients. A preliminary study, Neurol. Sci. 29 (2008) 3–9.
[13] Y. Cao, W.W. Tung, J.B. Gao, V.A. Protopopescu, L.M. Hively, Detecting dynamical changes in time series using the permutation entropy, Phys. Rev. E 70 (2004) 046217.
[14] B. Graff, G. Graff, A. Kaczkowska, Entropy measures of heart rate variability for short ECG datasets in patients with congestive heart failure, Acta Phys. Polon. B 5 (2012) 153–157.
[15] D. Zhang, G. Tan, J. Hao, Fractal random walk and classification of ecg signal, Int. J. Hybrid Inf. Technol. 1 (2008) 1–10.
[16] L. Zunino, M. Zanin, B. Tabak, D. Pérez, OA. Rosso, Forbidden patterns, permutation entropy and stock market inefficiency, Physica A 388 (2009) 2854–2864.
[17] J.N. Xia, P.J. Shang, J. Wang, W.B. Shi, Permutation and weighted-permutation entropy analysis for the complexity of nonlinear time series, Commun. Nonlinear Sci. Numer. Simul. 31 (2016) 60–68.
[18] M. Costa, A.L. Goldberger, C.K. Peng, Multiscale entropy analysis of complex physiologic time series, Phys. Rev. Lett. 89 (2002) 068102.
[19] M. Costa, AL. Goldberger, CK. Peng, Multiscale entropy to distinguish physiologic and synthetic RR time series, Comput. Cardiol. (2002) 137–140.
[20] M. Costa, AL. Goldberger, CK. Peng, JM. Hausdorff, Multiscale Entropy Analysis of Human Gait Dynamics, Physica A (2003) 53–60.
[21] M. Costa, A.L. Goldberger, C.K. Peng, Multiscale entropy analysis of biological signals, Phys. Rev. E 71 (2005) 021906.
[22] R.A. Thuraisingham, G.A. Gottwald, On multiscale entropy analysis for physiological data, Physica A 366 (2006) 323–332.
[23] C.K. Peng, M. Costa, A.L. Goldberger, Adaptive data analysis of complex fluctuations in physiologic time series, Adv. Aadapt. Data Anal. 1 (2009) 61–70.
[24] L. Zhang, G. Xiong, H. Liu, H. Zou, W. Guo, Bearing fault diagnosis using multi-scale entropy and adaptive neuro-fuzzy inference, Expert Syst. Appl. 37 (2010) 6077–6085.
[25] J.L. Lin, J.Y.C. Liu, C.W. Li, L.F. Tsai, H.Y. Chung, Motor shaft misalignment detection using multiscale entropy with wavelet denoising, Expert Syst. Appl. 37 (2010) 7200–7204.
[26] M. Costa, A.L. Goldberger, C.K. Peng, Multiscale entropy analysis: a new measure of complexity loss in heart failure, J. Electrocardiol. 36 (2003) 39–40.
[27] M. Costa, A.L. Goldberger, C.K. Peng, Multiscale entropy to distinguish physiologic and synthetic RR time series, Comput. Cardiol 29 (2002) 137–140.
[28] M. Costa, C.K. Peng, A.L. Goldberger, J.M. Hausdorff, Multiscale entropy analysis of human gait dynamics, Physica A 330 (2003) 53–60.
[29] Y. Yin, P. Shang, Detection of multiscale properties of financial market dynamics based on an entropic segmentation method, Nonlinear Dynam. 83 (2016) 1743–1756.
[30] J. Wang, P. Shang, X. Zhao, J. Xia, Multiscale entropy analysis of traffic time series, Internat. J. Modern Phys. C 24 (2013) 1350006.
[31] S.H. Bian, P. Shang, Refined two-index entropy and multiscale analysis for complex system, Commun. Nonlinear Sci. Numer. Simul. 39 (2016) 233–247.
[32] E.W. Bai, K.E. Lonngrn, Synchronization and control of chaotic systems, Chaos Solitons Fractals 10 (1999) 1571–1575.

[33] E.W. Bai, K.E. Lonngrn, Sequential synchronization of two Lorenz systems using active control, Chaos Solitons Fractals 11 (2000) 1041–1044.
[34] X. Yu, Variable structure control approach for controlling chaos, Chaos Solitons Fractals 8 (1997) 1577–1586.
[35] H.N. Agiza, M.T. Yassen, Synchronization of Rossler and Chen chaotic dynamical systems using active control, Phys. Lett. A 278 (2001) 191–197.
[36] S. Bhalekar, V. Daftardar-Gejji, Synchronization of different fractional order chaotic systems using active control, Commun. Nonlinear Sci. Numer. Simul. 15 (2010) 3536–3546.
[37] M. Rafikov, J.M. Balthazar, On control and synchronization in chaotic and hyperchaotic systems via linear feedback control, Commun. Nonlinear Sci. Numer. Simul. 13 (2008) 1246–1255.
[38] B. Podobnik, D. Horvatic, A.L. Ng, H.E. Stanley, P.C. Ivanov, Modeling long-range cross-correlations in two-component ARFIMA and FIARCH processes, Phys. A 387 (2008) 3954–3959.
[39] J.R.M. Hosking, Fractional differencing, Biometrika 68 (1981) 165–176.
[40] B. Podobnik, H.E. Stanley, Detrended cross-correlation analysis: a newmethod for analyzing two nonstationary time series, Phys. Rev. Lett. 100 (2008) 084102.
[41] B. Podobnik, P.Ch. Ivanov, K. Biljakovic, D. Horvatic, H.E. Stanley, I. Grosse, Fractionally integrated process with power-law correlations in variables and magnitudes, Phys. Rev. E 72 (2005) 026121.
[42] R.R. Nigmatullin, Universal distribution function for the strongly-correlated fluctuations: general way for description of different random sequences, Commun. Nonlinear Sci. Numer. Simul. 15 (2010) 637–647.
[43] V. Plerou, P. Gopikrishnan, B. Rosenow, L.A.N. Amaral, H.E. Stanley, Econophysics: financial time series from a statistical physics point of view, Physica A 279 (2000) 443–456.
[44] Y. Yin, P. Shang, Modified DFA and DCCA approach for quantifying the multiscale correlation structure of financial markets, Physica A 392 (2013) 6442–6457.
[45] Y. Yin, P. Shang, Modified multidimensional scaling approach to analyze financial markets, Chaos 24 (2014) 022102.
[46] Y. Yin, P. Shang, Comparison of multiscale methods in the stock markets for detrended cross-correlation analysis and cross-sample entropy, Fluct. Noise Lett. 13 (2014) 1450023.
[47] E. Fedorova, Interdependence of Emerging Eastern European Stock Markets: Acta Universitatis Lappeenrantaensis, Lappeenranta University of Technology, 2013, p. 498.
[48] Y. Yin, P. Shang, Modified cross sample entropy and surrogate data analysis method for financial time series, Physica A 433 (2015) 17–25.
[49] Y. Yin, P. Shang, G. Feng, Modified multiscale cross-sample entropy for complex time series, Appl. Math. Comput. 289 (2016) 98–110.
[50] G.S. Belzoni, R.M. Colombo, An n-populations model for traffic flow, Eur. J. Appl. Math. 14 (2003) 587–612.
[51] R.M. Colombo, Hyperbolic phase transitions in traffic flow, SIAM J. Appl. Math. 63 (2002) 708–721.
[52] A. Klar, Kinetic and macroscopic traffic flow models, Piano di Sorrento, Italy, 2002.
[53] B.S. Kerner, Experimental feature of selforganization in traffic flow, Phys. Rev. Lett. 81 (1998) 3797–3800.
[54] D. Helbing, B.A. Huberman, Coherent moving states in highway traffic, Nature 396 (1998) 738–740.
[55] D. Helbing, Traffic and related self-driven manyparticle systems, Rev. Modern Phys. 73 (2001) 1067–1141.
[56] M.Y. Choi, H.Y. Lee, Traffic flow and 1/f fluctuations, Phys. Rev. E 52 (1995) 5979–5984.
[57] K. Nagel, S. Rasmussen, Traffic at the Edge of Chaos, MIT, Massachusetts, 1994.
[58] W. Leutzbach, Introduction to the Theory of Traffic Flow, Springer, Berlin, 1988.
[59] BS. Kerner, The Physics of Traffic, Springer, New York, 2004.
[60] P. Shang, X. Li, K. Santi, Chaotic analysis of traffic time series, Chaos Solit. Fract. 25 (2005) 121–128.
[61] P. Shang, X. Li, K. Santi, Nonlinear analysis of traffic time series at different temporal scales, Phys. Lett. A 357 (2006) 314–318.
[62] P. Shang, M. Wan, K. Santi, Fractal nature of highway traffic data, Comput. Math. Appl. 54 (2007) 107–116.
[63] P. Shang, Y. Lu, K. Santi, Detecting longrange correlations of traffic time series with multifractal detrended fluctuation analysis, Chaos Solit. Fract. 36 (2008) 82–90.
[64] P. Shang, A. Lin, L. Liu, Chaotic SVD method for minimizing the effect of exponential trends in detrended fluctuation analysis, Physica A 388 (2009) 720–726.
[65] X. Li, Z. Gao, J. Zheng, B. Jia, Network analysis of the evolution of traffic flow with speed information, Internat. J. Modern Phys. C 21 (2010) 177–188.